

Pressurized H₂ rf Cavities in Ionizing Beams and Magnetic Fields

M. Chung,¹ M. G. Collura,¹ G. Flanagan,² B. Freemire,³ P. M. Hanlet,³ M. R. Jana,¹ R. P. Johnson,² D. M. Kaplan,³
M. Leonova,¹ A. Moretti,¹ M. Popovic,¹ T. Schwarz,¹ A. Tollestrup,¹ Y. Torun,³ and K. Yonehara¹

¹*Fermi National Accelerator Laboratory, Batavia, Illinois 60510, USA*

²*Muons, Inc., Batavia, Illinois 60134, USA*

³*Illinois Institute of Technology, Chicago, Illinois 60616, USA*

(Received 12 July 2013; published 29 October 2013)

A major technological challenge in building a muon cooling channel is operating rf cavities in multitesla external magnetic fields. We report the first proof-of-principle experiment of a high pressure gas-filled rf cavity for use with intense ionizing beams and strong external magnetic fields. rf power consumption by beam-induced plasma is investigated with hydrogen and deuterium gases with pressures between 20 and 100 atm and peak rf gradients between 5 and 50 MV/m. The low pressure case agrees well with an analytical model based on electron and ion mobilities. Varying concentrations of oxygen gas are investigated to remove free electrons from the cavity and reduce the rf power consumption. Measurements of the electron attachment time to oxygen and rate of ion-ion recombination are also made. Additionally, we demonstrate the operation of the gas-filled rf cavity in a solenoidal field of up to 3 T, finding no major magnetic field dependence. All these results indicate that a high pressure gas-filled cavity is a viable technology for muon ionization cooling.

DOI: [10.1103/PhysRevLett.111.184802](https://doi.org/10.1103/PhysRevLett.111.184802)

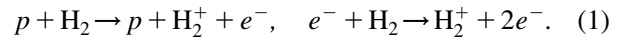
PACS numbers: 29.27.-a, 51.50.+v, 52.20.Hv, 52.40.Mj

Ionization cooling is a critical component for the realization of a neutrino factory and a muon collider, because only this cooling scheme can reduce the emittance of muon beams in times short compared to the muon lifetime [1,2]. A typical cooling channel will be composed of low- Z energy absorbers to reduce the momentum of the muon beam, normal conducting rf cavities to replace the lost longitudinal momentum, and strong confining magnets to focus the beam at the absorbers and compensate for the effect of multiple Coulomb scattering. In this channel configuration, strong static magnetic fields are present inside the rf cavities and increase the probability of rf breakdown [3,4]. Indeed, measurements at the Mucool Test Area (MTA) of Fermilab have shown that the achievable accelerating gradients for an 805 MHz vacuum pillbox cavity decreased from 40–60 MV/m to less than 20 MV/m in a 3 T solenoidal field (see Refs. [5,6] for details), which would seriously limit the performance of a cooling channel.

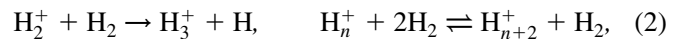
A rf cavity filled with high pressure hydrogen gas was proposed to overcome the above mentioned problem [7,8]. The gas provides the necessary momentum loss as a cooling material and also increases the breakdown gradient of the cavity. Since the collision frequency of electrons with H₂ molecules at 100 atm in rf fields $\nu_m \approx (2.6\text{--}29) \times 10^{13} \text{ s}^{-1}$ [9] is much higher than the cyclotron frequencies in the ambient magnetic fields $f_{ce} = 28 \times B[\text{T}] \times 10^9 \text{ s}^{-1}$, any effects of B are eliminated. Experiments have demonstrated that a breakdown gradient of 65.5 MV/m could be achieved in a 3 T magnetic field with 70 atm hydrogen gas [10].

Although these results are encouraging, a gas-filled cavity has not previously been tested with an ionizing

beam in the parameter range of interest. The beam (e.g., proton instead of muon for this experiment) will induce a number of reactions in the gas. It produces electrons and positive hydrogen ions through ionization processes



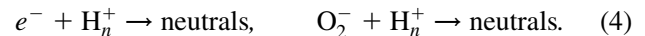
In the second reaction, we consider the fact that some of the electrons from the primary ionization can have enough energy to further ionize the gas. At high pressure, the positive hydrogen ions quickly transform into clusters [11,12]:



where $n = 3, 5, 7, \dots$. The free electrons and ions absorb energy from the rf field and transfer it to the gas through elastic and inelastic collisions. The addition of oxygen ameliorates this energy loss by capturing electrons in a three-body process, forming O₂⁻ [13]



The ions recombine through the processes [14,15]



We report here the measured rf power consumption by the electrons and ions in a gas-filled rf cavity in the MTA using a 400 MeV proton beam from the Fermilab linac (see Table I). This experiment is the first of its kind, which simultaneously involves an ionizing beam, high-pressure gas, high-power rf field, and strong dc magnetic field. We also estimate the electron capture time τ for reaction (3) as well as the recombination rates β_{ei} and β_{ii} for reactions (4), thus

TABLE I. Parameters of the present experiment at MTA and an envisioned practical cooling channel [16,17]. Symbols are explained in the text.

Parameter (units)	Present experiment at MTA (proton)	Practical cooling channel (muon)
p (atm)	20–100	180
E_0 (MV/m)	5–50	20
X_0 (V/cm/Torr)	0.5–10	1.5
B (T)	≤ 3	≤ 20
f (MHz)	~ 805	~ 805
Beam energy (MeV)	400	120
dE/dx (MeV cm ² /g)	6.24	4.43
Particles per bunch	$\leq 10^9$	10^{11} – 10^{12}
Pulse length (ns)	10^4	60
Bunch spacing (ns)	5	5
Synchronous phase, ϕ_s	random	159°
O ₂ concentration (%)	≤ 0.2	0.2

providing a complete picture of the plasma evolution, which is crucial for evaluating the feasibility of the gas-filled rf cavity.

Figure 1 shows the experimental apparatus including the gas-filled 805 MHz rf test cell (TC). The TC is made of copper-coated stainless steel. A pair of hemispherical copper electrodes is installed to concentrate the rf field around the beam path. The TC has a higher impedance than a typical cooling channel, which makes it ideal for studying plasma loading effects. The rf field is measured with a rf pickup loop. A 200-mm-long collimator with a 4-mm-diameter hole is placed upstream of the TC to get a well-defined beam profile. The beam position is monitored with a scintillating screen [18]. The incident proton intensity on the TC is measured by a toroid current transformer that is located in front of the TC. The initial density distribution of the plasma in the TC $\rho(r, z)$ is estimated from the numerical simulation code, G4beamline [19,20] [see Fig. 1 (inset)]. The calculated effect of the diffusion for the plasma in the transverse plane is negligible and we assume the plasma composition and density are controlled by τ , β_{ei} , and β_{ii} .

Figure 2 shows typical observed rf amplitudes for various conditions as a function of time. The rf pulse length is 40 μ s with a repetition rate of 15 Hz. Protons are sent to the cavity once the rf amplitude reaches the flattop value E_{\max} . We observe a rapid rf amplitude drop due to power consumption by the beam-induced plasma (blue curve in Fig. 2). Eventually, the rf amplitude reaches an equilibrium, where the rf source feeds an amount of power equal to that consumed by the beam-induced plasma and the cavity wall. When the beam is turned off, the rf amplitude starts to recover as the ionization process is stopped. The quality factor for this recovery is lower than that of the initial filling because the residual electrons and ions are still absorbing power. We note that the rf power reduction is significantly mitigated with the addition of an electronegative dopant gas [dry air (DA) in this case]. The gas-filled rf cavity was also demonstrated to operate

in a 3 T solenoid. As shown in Fig. 2, there is no dependence of the observed rf amplitude on magnetic field.

The production rate of ion pairs can be calculated by

$$\dot{N} = \dot{N}_b \times h \sum_k w_k \left(\rho_m \frac{dE/dx}{W_i} \right)_k, \quad (5)$$

where h is the propagation distance and w_k , ρ_m , dE/dx , and W_i are the abundance, mass density, stopping power, and average energy to produce an ion pair for the k th gas molecular species ($\sum_k w_k = 1$), respectively. The incident proton intensity into the cavity \dot{N}_b is typically $\sim 2 \times 10^{10}$ protons/ μ s, and \dot{N} is on the order of 10^{13} ion pairs/ μ s for this experiment.

Most ionization electrons slow down quickly through collisions with the ambient gas molecules and drift in phase with the applied rf electric field $E(t) = E_0 \sin(\omega t)$. The electrons reach an equilibrium temperature well above the ambient gas temperature by absorbing energy from the

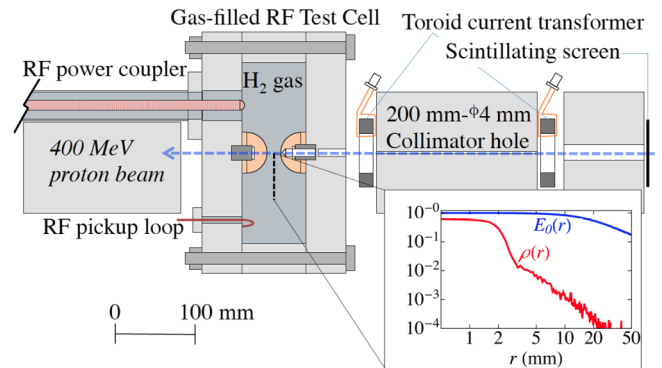


FIG. 1 (color online). Cross-sectional view of the experimental apparatus. Protons pass through the gas-filled rf TC as indicated and are stopped in a beam absorber placed downstream of the TC. All the equipment is mounted in the air-filled bore of a multitesla solenoid magnet (not shown). Radial distributions of the plasma density ρ and the electric field amplitude E_0 are plotted along the midplane of the TC (inset).

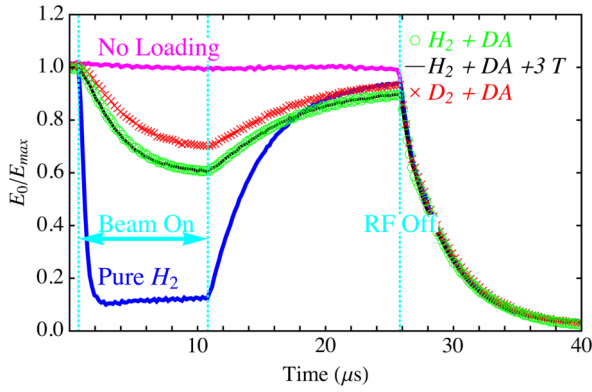


FIG. 2 (color online). Typical measured rf amplitudes vs time. The vertical lines indicate the timing of the beam and rf. The blue (magenta) curve corresponds to the case with (without) the beam in hydrogen gas. The doped cases represent 1% dry air (DA).

rf field and losing it through collisions with the gas molecules. The relaxation time is governed by the collision frequency between electrons and molecules and is estimated to be 0.3–70 ps for $E_0 = 50$ MV/m in 100 atm hydrogen gas [21]. Since this time scale is much shorter than the rf period ($T = 2\pi/\omega = 1/f$), it can be assumed that the electron equilibrium energy is determined by the instantaneous value of the electric field. In this case, we can estimate the electron contribution to the plasma loading by using the results of electron swarm experiments in a dc electric field [22], where it is found that the mobility of the swarm scales with the ratio of the field strength to the gas density. Here, we use $X_0 = E_0/p$, where E_0 is the peak rf field and p is the gas pressure at room temperature.

The rf power consumption due to the beam-induced plasma can be analytically formulated based on the above assumptions (with similar assumptions for the ions). As a convenient figure of merit, the mean rf power consumption per single ion pair in one rf cycle \overline{dw} is introduced as

$$dw = 2e \int_0^{T/2} [\hat{p}_e \mu_e + \hat{p}^- \mu_i^- + \mu_i^+] E_0^2 \sin^2(\omega t) dt, \quad (6)$$

where μ_e and μ_i^\pm are the mobilities of electrons and positive (negative) ions in a gas, which are functions of $X(t) = X_0 \sin(\omega t)$, p , and gas temperature. The coefficients \hat{p}_e and \hat{p}^- are the relative populations of the electrons and negative ions, respectively ($\hat{p}_e + \hat{p}^- = 1$). The value of μ_e is generally >100 times larger than that of μ_i^\pm . Therefore, the ionization electrons play the main role in loading the cavity. For low X , the value of μ_e is constant, but decreases for higher X because the electrons can excite the hydrogen molecules. In this case, dw should exhibit $\sim X_0^{1.6}$ dependence for a given pressure [23]. On the other hand, μ_i^\pm is constant over a wide range of X , as the ion temperature is equal to that of the ambient gas [24]. Consequently, dw for ions behaves as $\sim X_0^2$.

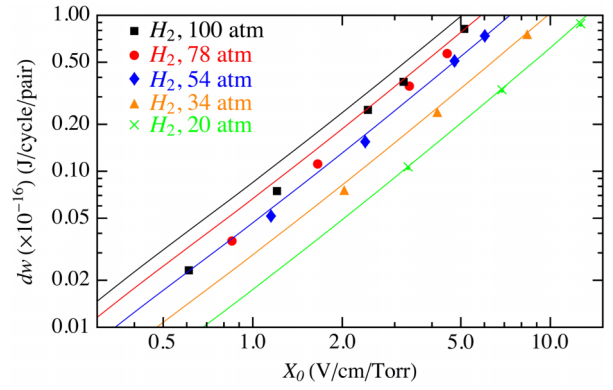


FIG. 3 (color online). Plot of \overline{dw} vs X_0 . The symbols represent the measured \overline{dw} and the lines are the \overline{dw} estimated from Eq. (6) for several hydrogen pressures. Each point is obtained by a statistical average over multiple measurements.

Using an equivalent circuit, the rf power consumption by the plasma can also be determined experimentally from the time evolution of the cavity voltage amplitude $V(t)$ (illustrated in Fig. 2) as

$$\Delta P = \frac{V(t)[V_{\max} - V(t)]}{R} - CV(t) \frac{dV(t)}{dt}, \quad (7)$$

where R , C , and V_{\max} are the shunt impedance and capacitance of the TC and the flattop rf voltage, respectively. If the total number of ion pairs N is known, the rf power consumption per single ion pair per rf cycle is estimated as

$$\overline{dw} = \frac{1}{g_c} \frac{\Delta P}{fN}, \quad (8)$$

where g_c corrects for the electric field variation over the plasma distribution [20].

In the case of pure hydrogen, the population of negative ions is assumed to be zero ($\hat{p}^- = 0$). For a short time after the beam turns on, we have found that the recombination processes have a negligible effect. In this case, N will be simply the time integral of the production rate given in Eq. (5). Figure 3 shows the measured \overline{dw} based on Eq. (8) as a function of X_0 for various hydrogen gas pressures. The solid lines are the predictions from Eq. (6) with the experimental data obtained from Ref. [22] for a dc field and low gas pressure. Our measurements are in good agreement with the predictions for the lowest pressure (20 atm), in which case \overline{dw} follows $X_0^{1.6}$. At higher pressures, the measured \overline{dw} 's become smaller than the estimated values. These deviations can be explained by the decrease in the electron drift velocity [25] mainly due to multiple scattering [26]. We do note that this pressure effect can lower the plasma loading for higher pressure operation of the cavity.

The rf power consumption was also measured in DA-doped hydrogen and deuterium gases as shown in Fig. 4. Oxygen, which constitutes 20% of DA, is an electro-negative gas. The lines in Fig. 4 represent the predicted dw

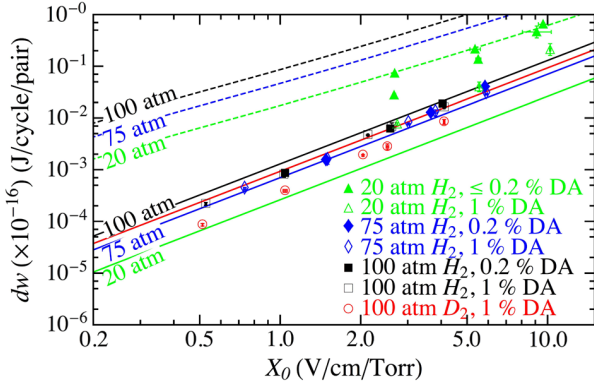


FIG. 4 (color online). Plot of \overline{dw} vs X_0 . The symbols represent the measured \overline{dw} for several gas pressures and DA doping concentrations. The solid (dashed) lines are the \overline{dw} estimated from Eq. (6) with $\hat{p}_e = 0$ ($\hat{p}^- = 0$).

values with the conditions that either \hat{p}^- is zero (upper three curves) or \hat{p}_e is zero (lower four curves). For the lower curves, it is assumed that the electrons are removed quickly by the capture process (3). We also assume in the lower curves that O_2^- and H_5^+ (D_5^+) are the main heavy ions contributing to \overline{dw} . The \overline{dw} measurements in Fig. 4 show an intermediate state at 20 atm, where some electrons still remain in the cavity. At 100 atm, on the other hand, the electrons seem to be completely removed; therefore, the \overline{dw} values follow the ion prediction curve. Further, \overline{dw} tends to vary as $\sim X_0^2$, which also supports the idea that the residual charged particles are heavy ions, not electrons. We emphasize that \overline{dw} is reduced by 2 orders of magnitude compared to the case of pure hydrogen, which significantly improves the performance of the gas-filled rf cavity. It is also interesting to note that \overline{dw} for the DA-doped deuterium case is smaller than that for DA-doped hydrogen (see open circles in Fig. 4 and crosses in Fig. 2). This is likely due to the dependence of the ion mobility on its mass.

The time evolution of charged particles can be estimated from the observed ΔP by using Eqs. (6)–(8) with \overline{dw} . The characteristic time for electron attachment to oxygen τ is evaluated from the time evolution of the observed electron density [23]. Figure 5 shows τ as a function of pressure with various DA concentrations. The value of τ is reduced at high pressure (i.e., $\tau \propto p^{-1.4 \text{ to } -1.6}$) and high DA concentration. The extrapolated τ in 1% DA (0.2% oxygen) at 180 atm is on the order of 0.1 ns, which indicates that the lifetime of an electron is much shorter than an 805 MHz rf period. The hydrogen recombination rate β_{ei} is estimated using a similar method as the τ analysis [23]. Note that g_c is time dependent in this analysis. The estimated β_{ei} range is 10^{-7} – 10^{-6} cm³/s. The rate of recombination between positive and negative ions β_{ii} has also been evaluated, although the exact ion species cannot be specified and so the overall rate is reported. Results indicate rates on the order of 10^{-9} – 10^{-8} cm³/s, and decrease with increasing pressure.

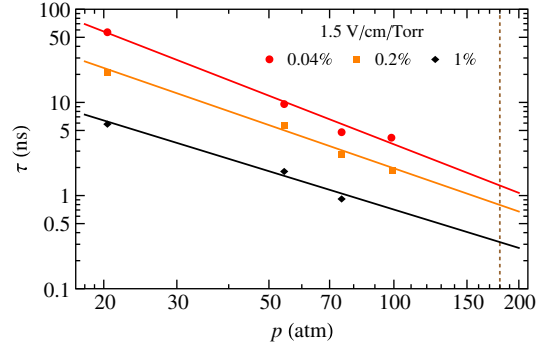


FIG. 5 (color online). Plot of τ vs pressure. The symbols represent the measured values in DA-doped hydrogen for several DA concentrations. The solid lines are fits to the data. X_0 has been chosen to correspond to a practical cooling channel E_0 and p (180 atm, shown by the dashed line).

Since the beam intensity is relatively low and the rf phase is not synchronized with the beam for the present experiment, we note that the voltage drops observed in Fig. 2 are mainly caused by the plasma loading, not by the conventional beam loading [27]. As the beam intensity increases for the practical cooling channel [16,17] (see Table I), both the plasma and beam loading increase. Since $v_m/f_{ce} \gg 1$ even for $B = 20$ T, and the plasma density is still much smaller than the gas density for the higher muon beam intensities, we do not expect any major change in the underlying physics of the plasma loading. Hence, the plasma evolution $N(t)$ and the corresponding drop in the accelerating voltage over the beam pulse $\Delta(V \sin \phi_s)$ can be readily estimated using Eqs. (7) and (8), and the extrapolated values of \overline{dw} , τ , β_{ei} , and β_{ii} . Preliminary studies [28] indicate that the plasma loading effects are smaller than the beam loading from the fundamental mode of the wakefields. For the beam intensities of 10^{11} – 10^{12} muons per bunch, $\Delta(V \sin \phi_s)_{\text{plasma}} / \Delta(V \sin \phi_s)_{\text{beam}} \approx 39\%$ – 41% . This strongly suggests that if the beam loading is mitigated by optimizing the beam and rf parameters (which is indeed a necessary condition for any practical cooling channel), the plasma loading can also be mitigated accordingly (as both loading effects are proportional to the beam intensity and shunt impedance). Detailed numerical simulations on these loading effects are planned [29,30] using the data obtained here to confirm the practicality of the gas-filled cavity.

In summary, we have experimentally demonstrated that the novel idea of operating a rf cavity after filling it with high-pressure gas (rather than keeping it under vacuum) can be a viable technology for muon ionization cooling. The extensive quantitative measurements presented in this work lay an important foundation for future cooling channel research and development based on gas-filled rf cavities.

The authors would like to thank R. Johnsen (University of Pittsburgh) for helpful comments and discussions.

Fermilab is operated by Fermi Research Alliance, LLC under Contract No. DE-AC02-07CH11359 with the U.S. Department of Energy. This work was partially supported by U.S. Department of Energy STTR Grant No. DE-SC00006266 and by grants from the U.S. Muon Accelerator Program (MAP) to Illinois Institute of Technology.

-
- [1] D. Neuffer, *Part. Accel.* **14**, 75 (1983).
- [2] M.M. Alsharo'a, C.M. Ankenbrandt, M. Atac, B.R. Autin, V.I. Balbekov, V.D. Barger, O. Benary, J.R.J. Bennett, M.S. Berger, J.S. Berg *et al.*, *Phys. Rev. ST Accel. Beams* **6**, 081001 (2003).
- [3] J. Norem, V. Wu, A. Moretti, M. Popovic, Z. Qian, L. Ducas, Y. Torun, and N. Solomey, *Phys. Rev. ST Accel. Beams* **6**, 072001 (2003).
- [4] R.B. Palmer, R.C. Fernow, J.C. Gallardo, D. Stratakis, and D. Li, *Phys. Rev. ST Accel. Beams* **12**, 031002 (2009).
- [5] A. Moretti, Z. Qian, J. Norem, Y. Torun, D. Li, and M. Zisman, *Phys. Rev. ST Accel. Beams* **8**, 072001 (2005).
- [6] J. Norem, A. Bross, A. Moretti, Z. Qian, D. Huang, Y. Torun, R. Rimmer, D. Li, and M. Zisman, in *Proceedings of PAC 2007* (IEEE, Piscataway, NJ, 2007), p. 2239.
- [7] R.P. Johnson *et al.*, in *AIP Conf. Proc.* **671**, 328 (2003).
- [8] R.P. Johnson, M.M. Alsharo'a, R.E. Hartline, M. Kuchnir, T.J. Roberts, C.M. Amkenbrandt, A. Moretti, M. Popovic, D.M. Kaplan, K. Yonehara *et al.*, in *Proceedings of LINAC 2004* (DESY/GSI, Lübeck, Germany, 2004), p. 266.
- [9] Y. Itikawa, *Phys. Fluids* **16**, 831 (1973).
- [10] P. Hanlet, M. Alsharo'a, R.E. Hartline, R.P. Johnson, M. Kuchnir, K. Paul, C.M. Ankenbrandt, A. Moretti, M. Popovic, D.M. Kaplan *et al.*, in *Proceedings of EPAC 2006* (EPS-AG, Mulhouse, France, 2006), p. 1364.
- [11] R. Johnsen, C.-M. Huang, and M.A. Biondi, *J. Chem. Phys.* **65**, 1539 (1976).
- [12] K. Hiraoka, *J. Chem. Phys.* **87**, 4048 (1987).
- [13] N.L. Aleksandov, *Sov. Phys. Usp.* **31**, 101 (1988).
- [14] R. Johnsen and S.L. Guberman, *Advances in Atomic, Molecular, and Optical Physics* (Academic, New York, 2010), Vol. 59, Chap. 3.
- [15] A. Fridman, *Plasma Chemistry* (Cambridge University Press, Cambridge, England, 2008), Chap. 2.
- [16] Y. Derbenev and R.P. Johnson, *Phys. Rev. ST Accel. Beams* **8**, 041002 (2005).
- [17] K. Yonehara, R.P. Johnson, M. Neubauer, and Y.S. Derbenev, in *Proceedings of IPAC, Kyoto, Japan, 2010*, p. 870.
- [18] M.R. Jana, M. Chung, B. Freemire, P. Hanlet, M. Leonova, A. Moretti, M. Palmer, T. Schwartz, A. Tollestrup, Y. Torun *et al.*, *Rev. Sci. Instrum.* **84**, 063301 (2013).
- [19] T. Roberts, *G4beamline* (Muons, Inc., Batavia, Illinois, 2013), <http://g4beamline.muonsinc.com>.
- [20] K. Yonehara, M. Chung, M. Jana, M. Leonova, A. Moretti, A. Tollestrup, B. Freemire, P. Hanlet, Y. Torun, and R. Johnson, in *Proceedings of IPAC, Shanghai, China, 2013*, p. 1481.
- [21] Y.P. Raizer, *Gas Discharge Physics* (Springer-Verlag, Berlin, 1991), Chap. 2.
- [22] J.J. Lowke, *Aust. J. Phys.* **16**, 115 (1963).
- [23] B. Freemire, Ph.D. thesis, Illinois Institute of Technology, 2013.
- [24] L. Viehland and E. Mason, *At. Data Nucl. Data Tables* **60**, 37 (1995).
- [25] R. Grünberg, *Z. Phys.* **204**, 12 (1967).
- [26] T.T. O'Malley, *J. Phys. B* **13**, 1491 (1980).
- [27] T. Wangler, *RF Linear Accelerators* (Wiley-VCH, Weinheim, 2008), Chap. 10.
- [28] M. Chung, B. Freemire, A. Tollestrup, and K. Yonehara, in *Proceedings of IPAC, Shanghai, China, 2013*, p. 1463.
- [29] K. Yonehara, M. Chung, A. Tollestrup, R. Johnson, T. Roberts, R. Ryne, B. Freemire, R. Samulyak, and K. Yu, in *Proceedings of IPAC, Shanghai, China, 2013*, p. 1478.
- [30] F. Marhauser (private communication).